Advanced Divertor Scenario in the Large Helical Device

S. Masuzaki, M. Shoji, M. Kobayashi, R. Sakamoto, T. Morisaki, M. Tokitani, H. Yonezu, T. Murase, N. Ohyabu, H. Yamada, A. Komori, O. Motojima
and the LHD experimental group

National Institute for Fusion Science, Toki 509-5292, JAPAN

e-mail contact of main author: masuzaki@LHD.nifs.ac.jp

Abstract. Neutral particle behavior in the Large Helical Device heliotron has been investigated to conduct the effective particle control using the intrinsic helical divertor. The torus in–out asymmetry was observed in the neutral pressure distribution, and the degree of the asymmetry depends on the divertor particle flux distribution, and thus, on the operational magnetic configuration. This asymmetry was well reproduced by the fully three-dimensional neutral transport code, EIRENE. Degradation of the plasma confinement with increasing of the neutral pressure was observed, and that suggests the effective particle control is necessary for the sustaining of long discharge with high performance plasma and the further improvement of the confinement. The modification of the open helical divertor to the closed one is planned for the particle control using helical divertor. It has been investigated using EIRENE code. Results of the calculation show that proper rearrangement of divertor plates and additional components, such as dome structure make the neutral particles to be compressed well in the divertor region, and effective divertor pumping to be possible. Based on the simulation and experimental results, design and installation of closed helical divertor is programmed in the Large Helical Device in the near future.

1. Introduction

Particle control using divertor is a key issue especially for the next generation fusion devices, such as ITER in which D-T burning and long pulse operation will be conducted. In the Large Helical Device (LHD) heliotron, performing the efficient particle control using divertor to improve the plasma confinement and to achieve long pulse discharges with high heating power is one of the major experimental goals. The plasma experiments have been conducted under two divertor configurations. One is the helical divertor (HD) [1-8] and the other is the local island divertor (LID) [9-12]. In the LID configuration, closed divertor module consisting of the neutralizer plates and the pumping duct is installed into the m/n = 1/1 magnetic island in the periphery of the confinement region generated by perturbation coils, and the inner and the outer separatrix of the island works as the last closed flux surface and the divertor legs, respectively. The own pump system is equipped in the LID system, and very high pumping efficiency was achieved [12]. As the result, the internal diffusion barrier formation was discovered in the discharges with LID [13]. However the heat flux on the neutralizer plates is so high for the small wet area that the plates frequently damaged [10]. On the other hand, HD is the intrinsic divertor field line structure in the heliotron-type magnetic configuration, and the wet area is much larger than that in LID. HD has been equipped no baffle structure and no divertor pump system at this stage (open HD). It has been observed that the increase of the neutral pressure in the vacuum vessel causes degradation of plasma confinement, and it has also been observed during long pulse discharge experiments that outgassing in the HD and/or impurities release from the HD causes the termination of discharge [14]. These observations suggest that the active particle control using HD is necessary for farther improvement of the LHD plasma performances.

Unlike the onion-skin like magnetic field line structure in the scrape-off layer (SOL) in the poloidal divertor configuration tokamaks, there are ergodic layer, magnetic island chains and laminar layer in the LHD SOL. The particle and heat load distributions on the divertor have

been investigated in the HD configuration in LHD, and it has been revealed that the distributions are non-uniform even in the helical direction [1,2]. Comparison of the experimental observation and the field lines tracing calculation shows that the magnetic field line structure on the divertor dominates the distributions. The magnetic field line structure can be visualized by using the profile of the connection length of magnetic field lines (L_c). In the HD case, long field lines with over several hundred meters L_c approach the last closed flux surface (LCFS), and the outflow particle and energy from the core plasma come to the divertor mainly along the long field lines [2]. The L_c profile on the divertor varies with operational magnetic configuration, such as radial magnetic axis position, R_{ax}, and thus, the particle and heat flux profiles on the divertor also vary with the configuration [2]. To reconstruct HD for active control of the neutral particles, the understanding of the neutral particle behavior and three dimensional transport simulations are necessary.

In this paper, the neutral particle behavior and its impact on the plasma confinement in the present HD configuration are presented in the next section, and the comparison of the experimental and simulation results using three dimensional neutral particle transport code, EIRENE, is also shown in the section. The design of the new divertor configuration has been conducted using the simulation code, and the results are presented in section 3.

2. Experimental observation and comparison between that and the simulation results

The nominal major and minor radii of the LHD plasma are 3.9 m and 0.6 m, respectively. The steady state magnetic field strength is 3 T. The materials of the first wall and divertor plates are SUS316L and isotropic graphite, respectively. Two pump chambers equipping with cryogenic pumps are connected to the LHD vacuum vessel, and their total pumping speed is about 260 m^3/s. To measure the neutral pressure distribution in the LHD vacuum vessel, ASDEX type fast ion gauges (FG) [16] and a cold cathode gauge (CG) were installed. Figure 1 shows their locations. Two FGs are installed to the torus inboard-side private region in the different horizontally elongated cross-section, respectively. A FG is installed to bottom private region in a near vertically elongated cross-section. The CG locates at the torus outboard-side in a horizontally elongated cross-section, and that is in the entrance of one pump chamber.

The distribution of the particle flux on HD is non-uniform, and it is modified with changing operational magnetic configuration, such as R_{ax}. In the case of so-called inward shifted configurations (R_{ax} < ~ 3.69 m), the dominant particle deposition region is torus inboard side. On the other hand, in the case of outward shifted R_{ax} configurations, the region moves to torus outboard side [2,4]. Figure 2 shows the line-averaged density ($n_{e,bar}$) dependence of the neutral

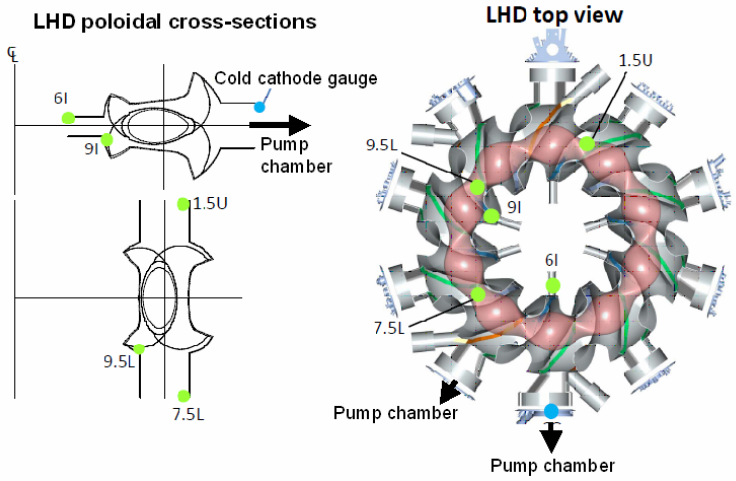

FIG. 1. Locations of the neutral pressure gauges. Green and blue circles are ASDEX type fast ion gauges and cold cathode gauge positions, respectively.

pressure measured by the gauges at the torus inboard and outboard sides for two R_{ax} cases. The $n_{e,bar}$ ranges from 1-30×10^{19} m^{-3}. The in-out asymmetry of the neutral pressure is clearly observed in the case of inward shifted magnetic configuration (Fig.2(a)) while the in-out asymmetry is reduced in the other case (Fig.2(b)). This result is considered to be caused by both the particle source distribution mentioned above and geometry of the LHD vacuum vessel. In the LHD vacuum vessel, there are helical coil cans, and their distance is narrower in the torus inboard side than that in the outboard side as shown in Fig.1. The neutral pressure is less than 0.1 Pa at the most even in the discharge in which $n_{e,bar}$ exceeds 10^{20} m^{-3}.

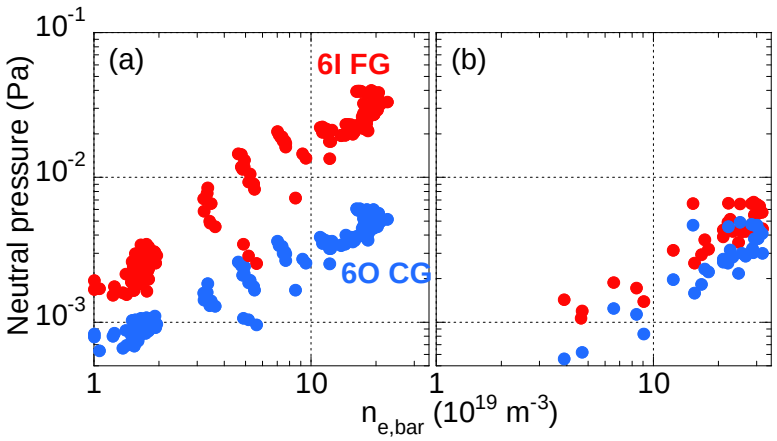

FIG. 2. Line averaged density dependence of the neutral pressure at torus inboard (red) and outboard (blue) sides. FG and CG are fast ion gauge and cold cathode gauge, respectively. (a) R_{ax} = 3.61 m, (b) R_{ax} = 3.95 m.

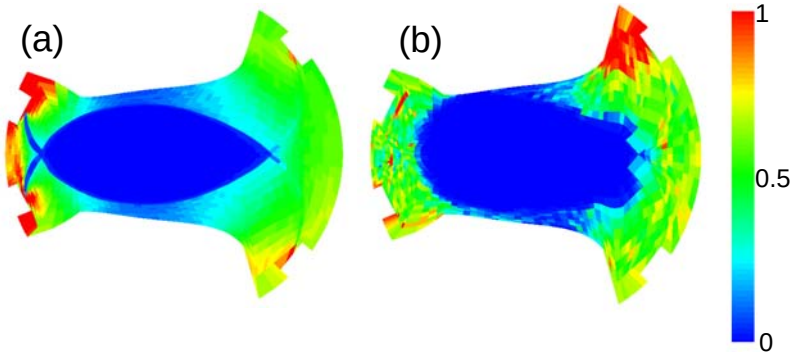

FIG. 3. Normalized hydrogen molecules density distributions calculated by using EIRENE code. (a) inward shifted and (b) outward shifted configurations, respectively. Left hand side is torus inboard side.

Three dimensional neutral transport code, EIRENE [17], has been utilized for analysis of the neutral particle behavior. Figure 3 shows the density distribution of hydrogen molecule in a horizontally elongated cross-section. The density is normalized by the maximum value. The in-out asymmetry in the inward shifted configuration and the reduction of the asymmetry in the outward shifted configuration are well reproduced by the calculation. The code was also examined by comparing with the spectroscopic observations of Hα intensity distribution, and the results of calculation agreed well with the observations [18].

Next, the impacts of the neutral pressure rise on the confinement properties are described. Figure 4 shows the time evolutions of the scaling parameter for energy confinement based on ISS95 scaling [19], the neutral pressure at torus outboard side and the line-averaged density during the discharge fuelled by the repetitive pellet injections [20]. Feedback control was applied to the pellet injection to sustain the line-averaged density to be 1×10^{20} m^{-3}. From t = 2 s, the density was kept to be the target density until t ~ 8 s. During almost constant density phase, neutral pressure gradually increased, and the time interval between pellet injections became long. It suggests that the recycling neutral particles increased. The energy confinement was degraded gradually as shown in Fig. 4, and it is considered to be caused by

the increase neutral pressure. Figure 5 shows that the evacuated hydrogen amount by the cryo-pumps mentioned above increases during a consecutive pellet fuelled discharges. That means the wall pumping capacity decreases shot by shot, and the neutral pressure during discharge increase. As the result, the line-averaged density rises with same fuelling. It is observed that the increase of neutral pressure prevents the formation of the internal diffusion barrier (IDB) [13]. These experimental observations suggest that the particle control necessary for further improved plasma confinement and sustaining the improved confinement with repetitive pellet fuelling.

3. Design of the closed helical divertor configuration

On the basis of the above mentioned experimental and simulation results, design of the closed HD (CHD) has been conducted. The target exhaust particle flux of the CHD is 10 Pa·m^3/s (H_2) which corresponds to the averaged fueling particle flux with the repetitive hydrogen ice-pellet injection (10 Hz, 1 Pa·m^3 (H_2)/pellet) preparing for steady state sustaining of the high density plasma. The neutral pressure in the HD region is rather low compared to that in tokamaks as mentioned in section 2. It is less than 0.1 Pa and 0.01 Pa at the torus inboard-side and the entrance of the pump chamber, respectively, even during high density, $n_{e,bar} > 1\times10^{20}$ m^{-3}, discharges with pellet injection. Unlike the poloidal divertor in tokamaks, the HD is not axisymmetrical, and the particle and the heat fluxes depositions are non-uniform even in the helical direction. Neutral particles recycled on the divertor plates can escape from the HD region because of the non-uniform plasma distribution and short field lines length from X-point to the divertor. Therefore, neutral pressure in the HD region is rather low. To achieve the target

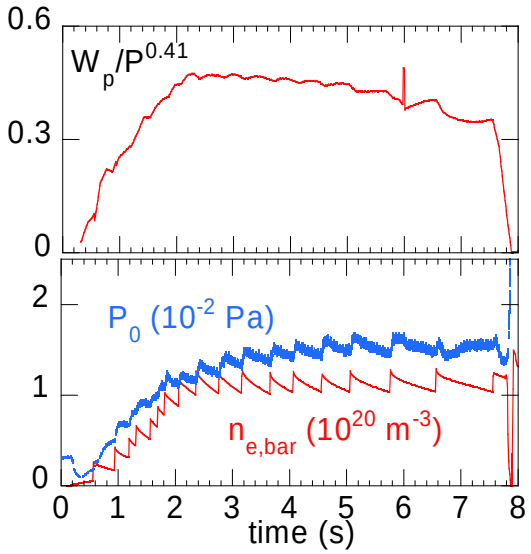

FIG. 4. Time evolutions of the scaling parameter for energy confinement based on the ISS95 scaling (top), neutral pressure measured by CG and the line averaged density (bottom). "W_p" is the plasma stored energy, and "P" is the heating power.

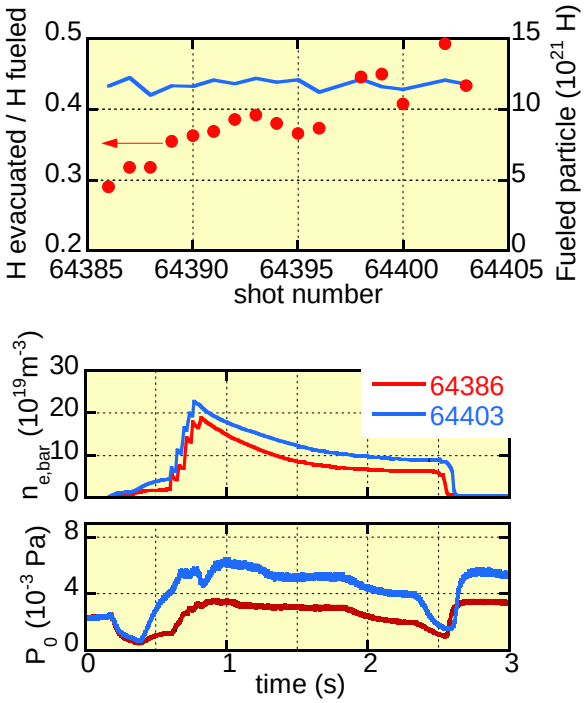

FIG. 5. The ratio of the amounts of evacuated to fuelled hydrogen particles and the number of fuelled hydrogen during consecutive pellet fuelled high density discharges (top). Time evolutions of the line-averaged density and neutral pressure during the first and last discharges in the series of the consecutive discharges (bottom).

exhaust flux using realistic pump system, such as in-vessel cryo pumps, the neutral pressure in the HD has to be 10 times risen, and the closure of the HD with proper structure is necessary for the pressure rise. For the first step to full closed HD, the torus-inboard side divertor is planned to be reconstructed first because the plasma confinement is better in inward shifted configuration than outward shifted one, and the dense divertor particle deposition appears at the torus inboard side divertor in the former configuration.

The exploring of the structure has been conducted using EIRENE code by trial and error [21]. In this calculation, the parameters of the background plasma were kept constant, and no plasma flow was taken into account. The operational magnetic configuration was R_{ax} = 3.6 m (inward shifted). It is required that there are enough space for installation of in-vessel pumps in the structure, and is also required that the structure is tolerant of the divertor heat load. The structure consisting of present divertor plates and additional baffle plates is the simplest one, and the compression of the neutral particles was examined first with this structure. In this case, the pumps were planed to be installed below the baffle plate. Figure 6 shows the calculated averaged hydrogen molecule density at the inboard side divertor region with and without baffle plates. Three spatial distances between the baffle plates, δ, were examined. It is shown that the neutral pressure rise with the installation of the baffle plates is up to 3 - 4 times larger than that in the open HD case, and the target pressure cannot be obtained in this

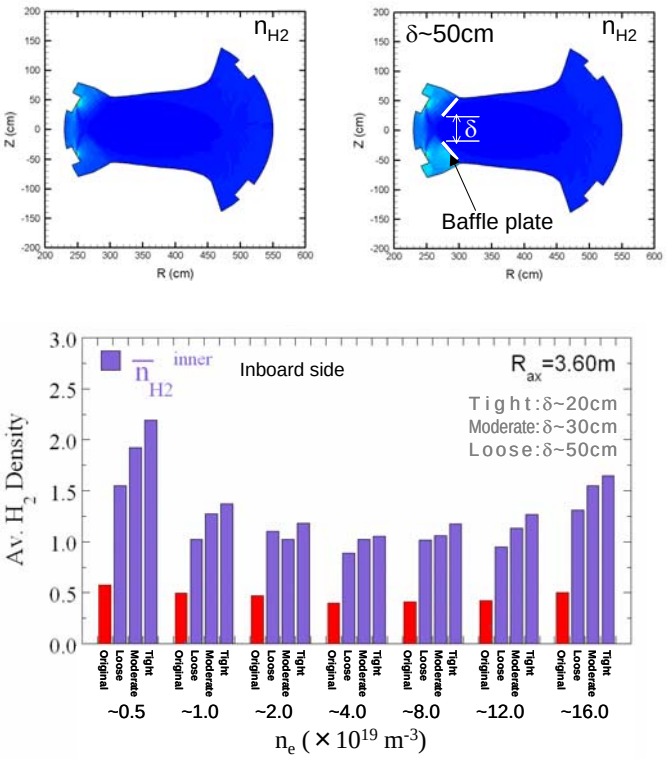

FIG. 6. (top) Density distributions of hydrogen molecule in a horizontally elongated cross-section with and without baffle plates. Spatial distance between the baffle plates is δ. (bottom) Averaged density of hydrogen molecule in the inboard side divertor region. Red bars indicate the density in the "open" divertor. Three δ (tight, moderate, loose) were examined.

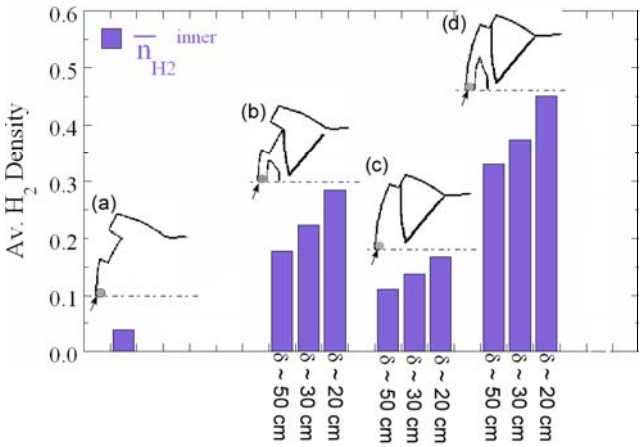

FIG. 7. Averaged hydrogen molecule density in various closed divertor structures which were examined. Insertions show the divertor structures in a holizontally elongated cross-section (above the equatorial plane); (a) open divertor (present structure) (b) (a) + dome and baffle plate (c) rearrangement of divertor plates + baffle plate. (d) (c) + dome. Baffle plates and dome are shown by white lines and blocks. δ is the width of throat of baffle plates.

structure. It is also shown that δ dependence of the density is not so strong. To achieve the target parameters, other ideas of CHD structure were examined. Figure 7 shows the averaged density of hydrogen molecule at the divertor region for different CHD structures. In Fig. 7, (a) is the present "open" HD structure. In the case of (b), divertor plates positions are same as (a), and baffle plates and dome structure are added. In the cases of (c) and (d), divertor plates are rearranged, and their surfaces are not faced to core plasma region to reduce direct loss of recycled particles. The difference between (c) and (d) is without and with the dome structure. From these calculations, we found that: 1) the width of throat of baffle plates, δ, affects the density weakly as same as the simplest case. 2) The main role of the dome structure seems to be reducing the volume of the divertor region. 3) Comparison of (b) and (d) shows that about two times higher density in (d) case for the rearrangement of the divertor plates.

Figure 8 shows both the present open HD and the latest design of CHD as the result of the exploring. In CHD, divertor plates face to torus-inboard vacuum vessel, and the dome structure is installed in the private region. The width of the throat of baffle plate is about 50 cm to avoid leading edge problems. Calculated distributions of hydrogen molecule density for both divertor structures are shown. In this case, the plasma parameters profiles in the HD region were calculated with a one-dimensional plasma fluid analysis using upstream plasma parameters from the calculation with EMC3-EIRENE code [8]. Assuming the plasma flow velocity at the surface of the divertor plates to be an ion sound speed and no transverse transport to the magnetic field lines, three differential equations for plasma density, momentum and energy are solved along the magnetic field lines on the divertor legs by using the Runge-Kutta method. In the closed HD, the density at

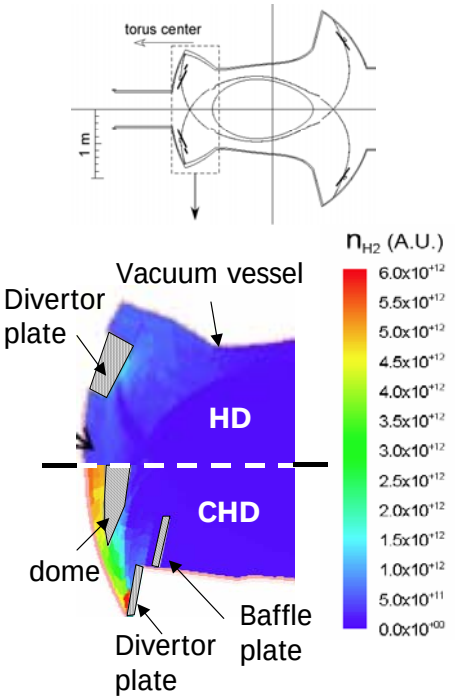

FIG. 8. (top) A horizontally elongated cross-section of the last closed flux surface (LCFS), boundary of ergodic layer, divertor legs and vacuum vessel in the open HD configuration. (bottom) Distributions of hydrogen molecules in the open HD and closed HD at torus-inboard side in the cross-section for the case of input power = 8 MW, electron density at LCFS = 4×10^{19} m^{-3}.

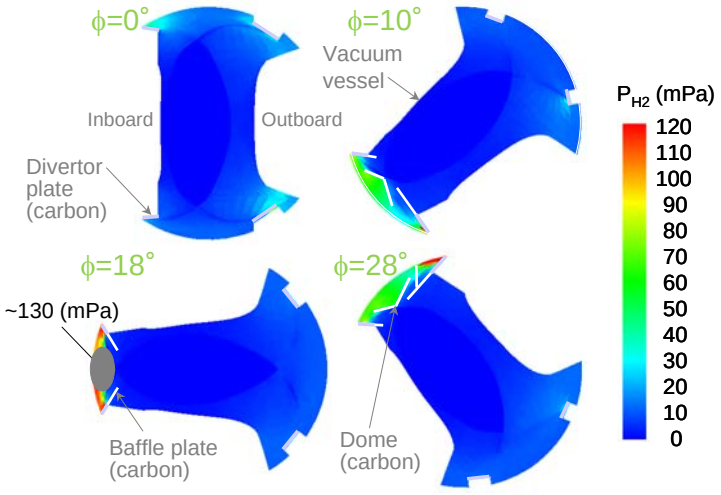

FIG. 9. Density distributions of hydrogen molecule in different poloidal cross-sections with the latest CHD configuration. Electron density at the last closed flux surface and the input power are assumed to be $6\times10^{19}m^{-3}$ and 8 MW.

the position where pump will be installed (space between the dome and inboard-side vacuum vessel in closed HD case) is about 20 times higher than that in present HD case, that means this closed HD design meets the target neutral pressure. Figure 9 shows the density distributions of neutral pressure in different poloidal cross-sections with the latest CHD configuration. The highest pressure is obtained below the dome at the horizontally elongated cross-section. In other cross-section, the pressure below the dome is about a half of the highest pressure.

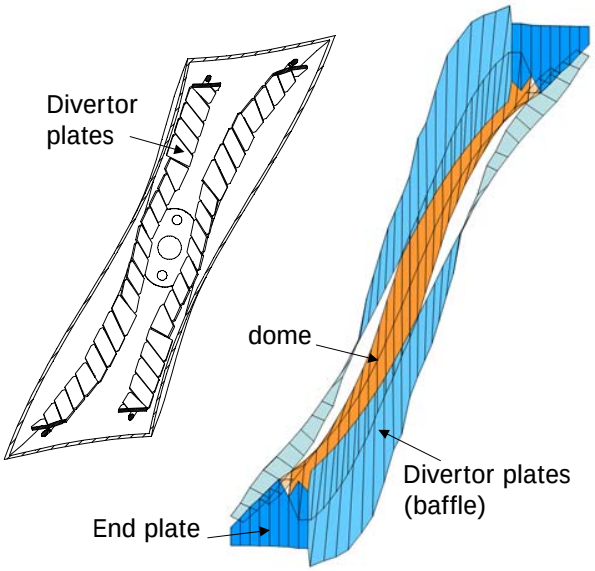

FIG. 10. Present (left) and new (right) divertor structures at the torus inboard side.

Based on the result of the calculation, the engineering design of CHD is in progress. Figure 10 shows the schematic views of the present and CHD structures at the torus inboard side. As mentioned above, the plasma facing surfaces of the divertor plates do not face to plasma but to first wall. The CHD region is plugged by the endplates, and the CHD forms a box like structure. In-vessel pumps are planed to be installed below the dome structure. The divertor plates will be made of isotropic graphite, and be cooled by water with the structure developed in advance [22]. One divertor plate consists of two isotropic graphite parts, and they are tightly fixed with bolt (Mo or TZM) M6 bolts lateral sandwiching a SS cooling pipe of 27.2 mm in diameter.

4. Summary

Neutral particle behavior in LHD heliotron has been investigated to conduct the effective particle control using the intrinsic helical divertor. The distribution of the neutral particles was investigated with neutral pressure gauges. The impact of the neutral pressure rise on the plasma confinement also investigated, and it was revealed that the pressure rise degrade the confinement. That suggests that the neutral particle control is necessary for achieving further improvement of the plasma confinement and sustaining long pulse discharge with high performance plasma.

The modification of the open helical divertor to the closed one in LHD has been investigated using fully three-dimensional neutral transport code EIRENE, to accomplish the active particle control to improve plasma confinement and to sustain high performance long pulse discharges. Results of the calculation show that proper rearrangement of divertor plates and additional components, such as dome structure make the neutral particles to be compressed well in the divertor region, and effective divertor pumping to be possible. Based on the simulation and experimental results, design and installation of closed helical divertor is programmed in LHD.

References

[1] OHYABU, N., et al., **"**The Large Helical Device (LHD) helical divertor**",** Nucl. Fusion **34** (1994)

[2] MASUZAKI, S., et al., " The divertor plasma characteristics in the Large Helical Device", Nucl. Fusion **42** (2002) 750.
[3] MORISAKI, T., et al., **"**Characteristics of Edge Magnetic Field Structure in LHD Heliotron", Contrib. Plasma Phys. **40** (2000) 266.
[4] MORISAKI, T., et al., " Effect of Magnetic Ergodicity on Edge Plasma Structure and Divertor Flux Distribution in LHD", Contrib. Plasma Phys. **42** (2002) 321.
[5] MASUZAKI, S., et al., "Helical divertor and the local island divertor in the Large Helical Device", Plasma Phys. Control. Fusion **44** (2002) 795.
[6] MASUZAKI, S., et al., " The relation between edge and divertor plasmas in the Large Helical Device", J. Nucl. Mater. **313-316** (2003) 852.
[7] KOBAYASHI, M., et al., "Divertor transport study in the large helical device", J. Nucl. Mater. **363-365** (2007) 294.
[8] FENG, Y., et al., "Fluid features of the stochastic layer transport in LHD", Nucl. Fusion **48** (2008) 024012.
[9] KOMORI, A., et al., "Edge plasma control by local island divertor in LHD", Nucl. Fusion **45** (2005) 837.
[10] MORISAKI, T., et al., "Local island divertor experiments on LHD", J. Nucl. Mater. **337-339** (2005) 154.
[11] KOBAYASHI, M., et al., "3D Divertor Transport Study of the Local Island Divertor Configuration in the Large Helical Device", Contrib. Plasma Phys. **46** (2006) 527.
[12] MASUZAKI, S., et al., "Divertor plasma and neutral particles behavior under the local island divertor configuration in the Large Helical Device", J. Nucl. Mater., **363-365** (2007) 314.
[13] OHYABU, N., et al., "Observation of Stable Superdense Core Plasmas in the Large Helical Device", Phys. Rev. Lett. **97** (2006) 055002.
[14] SAITO, K., et al., " ICRF long-pulse discharge and interaction with a chamber wall and antennas in LHD", J. Nucl. Mater. **363-365** (2007) 1323.
[16] HAAS, G., et al., "Measurements on the particle balance in diverted ASDEX discharges", J. Nucl. Mater. **121** (1984) 151.
[17] REITER, D., et al., "The EIRENE and B2-EIRENE Codes", Fusion Sci. Technol. **47** (2005) 172.
[18] SHOJI, M., et al., "Three-dimensional neutral particle transport simulation for analyzing polarization resolved H-alpha spectra in the large helical device", J. Nucl. Mater. **363-365** (2007) 827.
[19] STROTH, U., et al., "Energy confinement scaling from the international stellarator database", Nucl. Fusion **36** (1996) 1063.
[20] SAKAMOTO, R., et al., " Repetitive pellet fuelling for high-density/steady-state operation on LHD", Nucl. Fusion **46** (2006) 884.
[21] SHOJI, M., et al., "Optimization of Closed Divertor Configuration for Effective Particle Control in LHD Plasmas", Contrib. Plasma Phys. **48** (2008) 185.
[22] KUBOTA, Y., et al., "Design and thermal performance of an improved mechanically attached module for divertor plate of LHD", Fusion Eng. Des. **75-79** (2005) 297.